UNIVERSITY OF CALIFORNIA, SAN DIEGO

Thermo-responsive Hydrogel Desiccant Material

A Thesis submitted in partial satisfaction of the requirements
for the degree Master of Science

in

Engineering Sciences
(Mechanical Engineering)

by

Patrick William Charles

Committee in charge:

Professor Renkun Chen, Chair
Professor Shengqiang Cai
Professor Carlos Coimbra

2017

The Thesis of Patrick William Charles is approved, and it is acceptable in quality and form for publication on microfilm and electronically:

_____

_____

_____

Chair

University of California, San Diego

2017

DEDICATION

This thesis is dedicated to my grandfather, Rudolph Pipa, who encouraged my interest in science at a young age, and who urged me to stay in school as long as I could handle! Thanks also go to my parents who have guided and aided me in my decisions my entire life, and to my fiancée Erin Strand, who has supported me through the late nights, stress, and doubt that grad school brings.

TABLE OF CONTENTS

LIST OF FIGURES

LIST OF TABLES

ACKNOWLEDGEMENTS

This research would not have been possible without the support and guidance of Prof. Renkun Chen. The development of hydrogel synthesis techniques was led by Shuang Cui, and the experimental design was carried out in partnership with Shuang as well. Thanks also to Rentian Dong and Evan Mueller for their help in the lab, and for always asking questions to be sure Shuang and I actually know what we are talking about!

Chapter 3, in part, has been submitted for publication of the material as it may appear in ”Thermo-responsive desiccant with high adsorption capability and low regeneration temperature for energy efficient cooling.” Cui, Shuang; Charles, Patrick; Chen, Renkun.

Chapter 4, in part, has been submitted for publication of the material as it may appear in ”Thermo-responsive desiccant with high adsorption capability and low regeneration temperature for energy efficient cooling.” Cui, Shuang; Charles, Patrick; Chen, Renkun.

ABSTRACT OF THE THESIS

Thermo-responsive Hydrogel Desiccant Material

by

Patrick William Charles

Master of Science in Engineering Sciences
(Mechanical Engineering)

University of California, San Diego, 2017

Professor Renkun Chen, Chair

Desiccant based dehumidification allows for independent treatment of latent and sensible properties in air conditioning systems and enables the use of energy-saving solar thermal evaporative cooling systems. These systems can reduce dependence on vapor-compression air conditioning which is a significant source of greenhouse gases. Recent research has focused on polymer-based desiccant materials which have higher adsorption capacities than conventional materials such as silica gel and zeolite. Solid desiccant materials used in dehumidification systems are typically utilized in a cycle in which they absorb water vapor from a process air stream and are then regenerated by a source of

hot, dry air which evaporates and removes water contained in the material, allowing it to again absorb water from the process air. This research focuses on the development and testing of a hygroscopic salt impregnated, NIPAM hydrogel-based thermo-responsive desiccant material that can be regenerated by elevating the material to its lower critical solution temperature (LCST), enabling a significant energy saving over materials that require regeneration through water evaporation. At this LCST, the water adsorbed by the desiccant becomes insoluble in its NIPAM polymer matrix and is removed through droplet formation induced by gravity. Adsorption and regeneration testing was performed on the material to evaluate the feasibility of using this temperature-sensitive desiccant into a dehumidification system. Testing shows this composite material has a maximum SR of > 2 and analysis indicates improvement in regeneration heat requirements over existing desiccant materials.

Chapter 1

Introduction

1.1 Cool Runnings

When most people walk into an air conditioned building on a hot, sticky summer day, they typically remark at how much cooler it is.“Thank god for A/C”, one might say, “It’s so much cooler in here!” A thermometer will indeed read a lower temperature inside the air conditioned space, but a major component of the comfort we experience when entering into an air conditioned space is due to the humidity, or the relative presence of water vapor in the air. Anyone who has experienced a particularly hot summer day in St. Louis, Missouri can tell you that it feels quite different from a day of the same temperature in Phoenix, Arizona. Dry air allows our bodies to cool through perspiration much more easily than in humid environments. The energy associated with the changes in air humidity is referred to as “latent” energy transfer (from the Latin *latens* meaning concealed or hidden [1]), whereas changes in temperature are referred to as “sensible” energy changes, i.e. changes that are easily perceived or sensed.

This range of latent properties in air affects not only the people in the room or space, but also the conditioning system by which the air is delivered. The air conditioning

system most people encounter in their daily lives is known as a vapor-compression based air conditioning system, which uses a loop of low-boiling point liquid (known as a refrigerant) in a heat pump system to move heat from one place to another. These systems deliver conditioned air in a single step: the cold air conditioning coils cool and dry the air, causing the water vapor contained in air to condense. In particularly hot and humid areas, the air must be cooled to the point at so significantly that often the air being delivered from the air conditioner must be heated back up, in order to deliver it at an appropriate comfort level for the building occupants.

One way of exercising independent latent and sensible control over air conditioned air is by using desiccant dehumidification systems to dry the air. Not only does this eliminate the need for re-heating when VCAC (vapor compression air conditioning) systems are used, but it also enables other cooling technologies which will be discussed later in the report, including solar-regenerated evaporative cooling systems. Another concern with VCAC systems is that they utilize refrigerants which are significant greenhouse gases when released. The United States has restricted the use of the more harmful refrigerants such as hydrofluorocarbons (HFCs) in the past few decades, but the use of VCAC systems continues to grow worldwide.

All desiccant dehumidification systems need to be regenerated, which is usually accomplished by using a heat source of some sort. This dehumidification method is particularly attractive due to the possibility of using waste heat sources or solar to regenerate the material. The downside to most of these desiccant materials, is that they require as much energy input into the material as is removed from the process air stream (in the form of a reduction of air enthalpy). In other words, some quantity of moisture from the air is removed, but the same amount of moisture must then be removed from the desiccant material.

If absorbed moisture could be removed from the desiccant by some other means,

or if the the energy needed to do so could be reduced, the overall efficiency of the system could be improved. A potential method of achieving this is by using a thermally sensitive hydrogel polymer as a desiccant base material. Some highly networked polymers have a characteristic called the lower critical solution temperature (LCST), above which there is a discontinuity in the miscibility of the polymer matrix that has dissolved a polar solvent. In simple terms, the polymer network of the hydrogel is in solution with water, but above this LCST, the polymer becomes insoluble. This material can be thought of as a sponge that squeezes itself out when it is raised to a certain temperature. If a dehumidification system were able to be created based on this material, it would be possible to regenerate the material by simply bringing it up to its LCST, rather than needing to supply enough energy to evaporate the water from the desiccant.

1.2 Objectives

The main objective of the thesis project is to investigate the performance and feasibility of the use of a temperature-sensitive polymer hydrogel material as the basis for a desiccant based dehumidification system. The goal is to determine whether this material is worth pursuing as a next-generation solid desiccant material, and also to explore the critical parameters which affect the desiccant performance. Additionally, the potential form factor and applications of the desiccant material into a dehumidification system will be considered:

1. Identify a suitable temperature-sensitive desiccant material
2. Explore the critical parameters which affect the desiccant materials performance
3. Characterize the dehumidification and regeneration behavior of the material

4. Estimate the improvements in energy performance that could be achieved by utilizing a temperature-sensitive desiccant material in an evaporative cooling system

Chapter 2

Background

2.1 Motivation for Alternative Air Conditioning Systems

Buildings are the largest consumer of primary energy in the United States at 41 % of total energy use. Industry and transportation make up the other 59 %. Additionally, 14.8 % of that energy use is in space cooling, surpassed only by space heating at 22.5 % of building energy use. This energy used in building cooling contributes to 6 % of the United States' overall carbon footprint. [2] Over 90 % of that building cooling is provided by vapor compression systems, which have global warming implications beyond the carbon footprint. [3] The impact of a certain gas on the capture of additional heat from the sun can be represented as global warming potential (GWP), where carbon dioxide has a GWP of 1. The refrigerants used in VCAC systems have a GWP of up to 10,000, meaning they would capture up to 10,000 times more heat than carbon dioxide would over a 100 year time period. [4, 5] Contributions to greenhouse gases due to refrigerants in the United States is currently low (< 1 %) but it is estimated that they will contribute to 9-19 % of greenhouse gas emissions worldwide by 2050. [6]

Vapor compression air conditioning systems are a major contributor to greenhouse

gases and global warming worldwide, both due to the energy consumed and due to the global warming potential of refrigerants. Building cooling is unlike other industries in that there lacks a concerted effort to make the technology more environmentally friendly. There are efforts to expand the use of renewable energy sources such as wind and solar and the U.S. government has required automakers to improve the efficiency of their vehicles. [7] Therefore, building cooling represents an opportunity to make an impact in slowing global warming.

Another issue with using VCAC is the difficulty in dealing with high latent loads. In air conditioning systems, there is a metric called the Sensible Heat Ratio (SHR) which indicates the fraction of energy that is put into changing the temperature in an air conditioning process (sensible heat) compared to the energy used to change the humidity of the air (latent heat):

$$\text{SHR} = \frac{\text{Sensible Heat}}{\text{Sensible Heat + Latent Heat}}$$

VCAC systems are typically only able to deliver air and human comfort conditions when the SHR is greater than 0.75. [8]

One of the more prominent alternatives to VCAC systems is desiccant based air conditioning, which uses material that absorbs water vapor fromt the air to dry the air for latent control. The use of desiccants also enables the use of solar-thermal evaporative cooling.

2.2 Desiccant Materials in Air Conditioning Systems

2.2.1 Desiccant Based Dehumidification

The use of desiccant materials in the United States to control air humidity dates back at least to the 1930s [9], with desiccants being used primarily in industrial settings to protect corrosion-sensitive materials and equipment. Desiccant-based air conditioning systems also found early applications in hospitals and other facilities where climate control was critical to the prevention of pathogen spread and growth. One of the earliest descriptions of the application of a regenerable desiccant air conditioning system is described by Dannies in 1959 [10], who described a building which passively circulated outside air through desiccant materials in the walls in order to dry the air and achieve an evaporative cooling effect. In the late 1970s, researchers in the U.S. began to research desiccant dehumidification systems in earnest, an early example of this is shown in Shelpuk and Hooker's 1979 report for the Department of Energy [11]. The report describes the axial flow desiccant rotor (Figure 2.1), which is now a common dehumidification bed form. This rotor consists of a cylinder with many small air channels whose walls are coated with desiccant material, most commonly silica gel. In a typical dehumidification system, the ducting sent to the desiccant rotor is split into two sections: a process air stream and a regeneration or reactivation air stream. The process air stream contains air which is to be dehumidified and cooled, while the regeneration air stream delivers heated air to remove the stored moisture taken from the process air stream. The desiccant rotor slowly rotates so the entire cylinder of material is gradually regenerated as it is used for dehumidification.

One of the most common implementations of the desiccant rotor is in a solar-regenerated desiccant evaporative cooling system. A diagram of a typical system can be seen in Figure 2.2. In this arrangement, ambient air is first passed through a desiccant

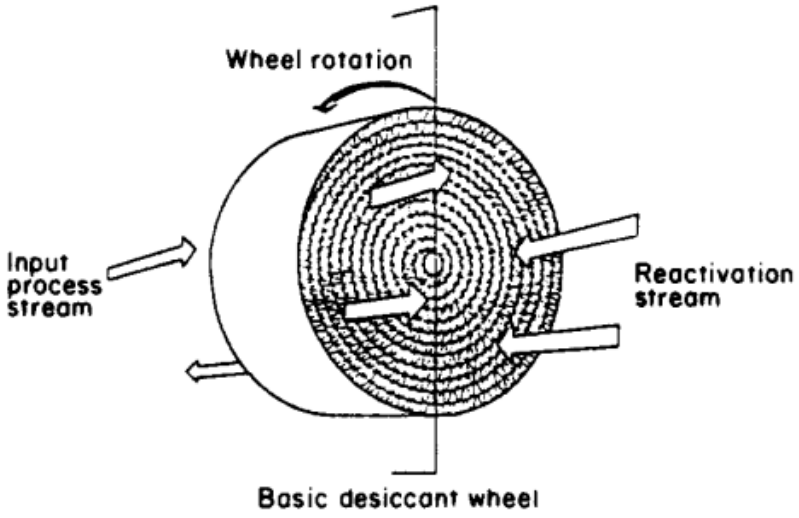

Figure 2.1: Diagram of an axial flow desiccant wheel [11]

rotor to dehumidify ambient air to achieve a desired humidity level. The dehumidified air is then passed through an evaporative cooler which takes advantage of water's high latent heat of vaporization to cool the air. This system utilizes a solar collector and thermal storage loop to transfer solar heat and use it as a regenerating heat source for the desiccant wheel (typical regeneration temperatures range from 60-100 °C [12]), and then this hot, humid air is exhausted to ambient.

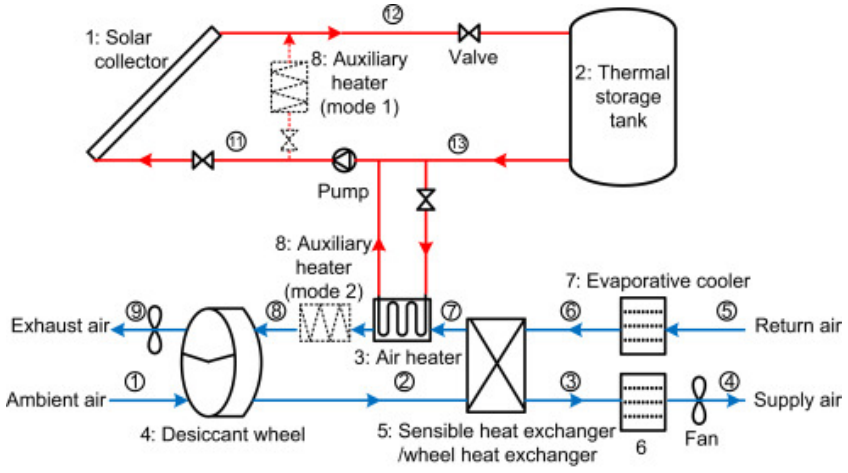

Figure 2.2: Schematic of a solar regenerated desiccant evaporative cooling system [12]

The coefficient of performance (COP) is a critical parameter in quantifying the performance of air conditioning systems. This factor is a ratio of the air conditioning work performed on the process air, divided by the amount of energy needed to provide that work. Since air conditioning systems typically operate like heat pumps, this COP is not a strict efficiency metric, and can have a value > 1. Referencing the numbered labels in Fig 2.2, the COP is defined:

$$COP = \frac{\dot{m}_p(h_1 - h_4)}{\dot{m}_r(h_8 - h_7)}$$

In this case, $\dot{m}_p$ is the mass flow rate of the process air (points 1 through 4) and $\dot{m}_r$ is the mass flow rate of the regeneration air (points 5 through 9). The enthalpy at each point in the diagram is denoted by h. When comparing desiccant wheel materials, it is helpful to define a desiccant COP, or DCOP, to directly compare desiccant performance without considering the effect of the air conditioning method (evaporative cooler, VCAC, etc.) Again referencing the numbered labels in Fig 2.2:

$$DCOP = \frac{\dot{m}_p(h_1 - h_2)}{\dot{m}_r(h_8 - h_7)}$$

2.2.2 Conventional Desiccant Materials

Materials such as silica gel and zeolite rely on van der Waals forces to adsorb water vapor are referred to as 'physical' adsorbers. The materials' high porous surface area provides capture sites for water vapor. The Shelpuk report [11] identifies silica gel and molecular sieves as good candidates for desiccant materials, the equilibrium water absorption curves in Figure 2.3 show the equilibrium water adsorption behavior at different relative humidity levels. The ideal desiccant material has a high water adsorption capacity at low relative humidity levels over a wide range of air temperatures. Silica gel

has a high adsorption capacity relative to other desiccants in its class (Figure 2.3a), but it drops off at higher temperatures (Figure 2.3b) which limits the temperature range of process air it can dehumidify. Due primarily to its low cost and high cycle life, it is one of the most commonly used desiccants in dehumidification systems. [13]

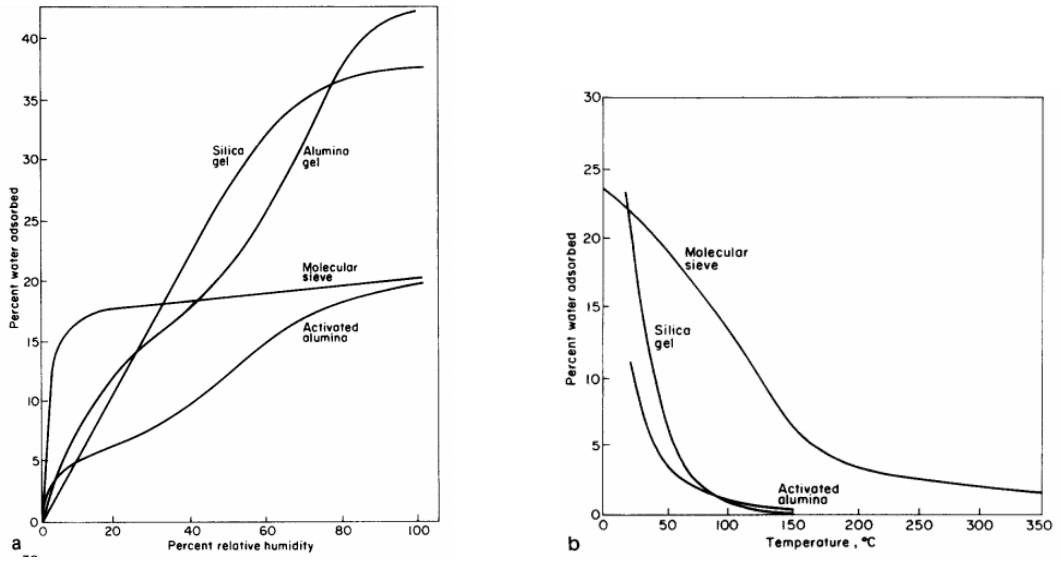

(a) Equilibrium adsorption vs Relative Humidity

(b) Equilibrium adsorption vs temperature (1.4 kPa water vapor pressure)

Figure 2.3: Equilibrium water adsorption curves for various desiccant materials [11]

2.2.3 Composite Desiccants

In general, materials with higher adsorption capacities give higher dehumidification performance because they are able to dry the air much more effectively and use less material in order to achieve the desired humidity level. In 1996 Levitskij *et al.* [14] synthesized a composite desiccant by impregnating a host matrix with a hygroscopic salt for improved desiccant performance and noted improved water absorption capacity over existing materials such as silica gel or zeolites. One of the challenges of depositing a salt in a silica gel matrix is the issue of the formation of salt solution films which inhibit performance. Silica gel relies on its high surface area to provide sites for water

adsorption and a liquid film over the pores reduces adsorption performance. Zhang *et al*. characterized this problem, indicating an optimum salt concentration which did not have a salt film layer and also had the best desiccant performance. [15] Gong *et al*. found that finding an optimum salt concentration is not sufficient; taking care to impregnate the gel evenly with solution provided for high cylclic performance. The film layer formation issue was solved by exposing the composite desiccant to a humid environment and allowing the salt solution to be washed off.

Jia *et al*. used a LiCl impregnated silica gel desiccant wheel to achieve a DCOP (desiccant COP) of 3.2 at 80 % RH, compared to DCOP of 1.8 for silica gel wheel at the same conditions. [16]. Xu *et al*. created a $CaCl_2$-polyacrylate desiccant which achieved SR > 2.1 at 90 % RH, but found challenges with material structural stability. [17] Yang *et al*. developed a composite hydrogel desiccant based on sodium polyacrylate and LiCl which achieved an equilibrium SR of 280 % at 99 % RH. [18]. Also notable in Yang's 2015 publication is the tendency for the material to continue absorbing water in a highly humid environment $\left(> 99\ \%\right)$. The composite material appeared to reach an equilibrium absorption capacity in 6 h, but continued to swell past 24 h. This behavior is due to the high swelling capacity of the sodium polyacrylate material, which is able to diffuse water through the hydrogel matrix over time. Polymer hydrogel materials are promising for desiccant applications, since their ability to store water in a matrix allows for much higher adsorption capacities.

2.3 LCST Materials

In solvent-polymer systems, the miscibility of the polymer is determined by the resultant thermodynamic Gibbs free-energy of the mixture, which is a function of both mixing enthalpy and entropy: $G = H - TS$. A homogeneous solution can be obtained

when the free energy of mixing $\Delta G_m < 0$, that is the free energy of the mixed solution G_{12} is less than the free energy of the independent components.

$$\Delta G_m = G_{12} - \left(G_1 + G_2\right) < 0$$

In general, the free energy of mixing decreases with increasing temperature up to the critical point of the solvent. The minimum temperature where a single mixed phase occurs is known as the upper critical solution temperature (UCST). In polymer/polar solvent solutions, there is an additional two phase region that can occur far below the solvent critical temperature, known as the lower critical solution temperature. Above this temperature the polar bonding made between polymer and solvent becomes energetically unfavorable and the solution separates into two phases, one consisting primarily of the solvent and the other consisting primarily of the polymer. [19]

This ability to control the mixed phase of a polymer has made LCST materials particularly attractive for applications like controlled drug delivery and soft robotics. Hydrogel materials have been found to respond to a variety of stimuli besides temperature including voltage, pH, and chemical concentrations. [20, 21] Chen *et al.* utilized this effect to develop a vapor sensor based on NIPAM and $CaCl_2$. [22]. Zheng *et al.* developed a mechanically tough NIPAM hydrogel based bilayer beam that can be actuated with a change in temperature. [23] Yang *et al.* described a method of impregnating cotton fibers with a thermo-responsive hydrogel which adsorbs water which could be used to capture fog in the evening in areas with low annual rainfall. [24] The water is then released from composite cotton-gel through a temperature change and captured for use.

2.4 Thermodynamics of Desiccants

2.4.1 Adsorption

Desiccant materials capture water vapor from air through a variety of methods. The equilibrium partial pressure of adsorbed water vapor can be described by the Gibb's adsorption equation:

$$\frac{\partial\left(\ln p\right)}{\partial T} = \frac{\left(h_g - h_s\right)}{RT^2}$$

In physical adsorbents like zerolite or silica gel, the adsorption of water vapor is energetically favorable due to the high surface area of the material. The water is able to form a stable monolayer on the surfaces presented by the silica gel. Chemical desiccants such as hygroscopic salts have a chemical affinity for water vapor, and the absorption process can be described by the following:

$$\mathrm{H_2O(g) = H_2O(l)}$$

$$\mathrm{H_2O(l) + nCaCl_2 = NCaCl_2(aq)}$$

There is heat release associated with both the phase transfer from gas to liquid Δh_g $\left(\mathrm{g\ to\ l}\right)$ and a heat of solution Δh_{sol} for the dissolution of the salt into an aqueous solution. [25] Both of these enthalpies must be taken into consideration when calculating the thermodynamics of absorption for chemical desiccants.

2.4.2 Regeneration

The U.S. Department of Energy presents an analysis of the theoretical regeneration heat of a desiccant material in its BEETIT Funding Opportunity Announcement

document [26], which is represented below. An additional analysis is presented later in this work, to show the theoretical regeneration heat of the LCST hydrogel desiccant. The minimum amount of work needed to dehumidify air to specified conditions is W_l, in units of work per unit mass of dry air:

$$W_l = R_{air} T_{amb} \ln\left(\frac{P - P_{vapor}}{P_{vapor_{amb}}}\right) + x R_{vapor} T_{amb} \ln\left(\frac{P_{vapor}}{P_{vapor_{amb}}}\right)$$

In the equation, R_{air} and R_{vapor} are the gas constants of air and water vapor, T_{amb} is the temperature of the ambient air, P is the ambient pressure of air, P_{vapor} and $P_{vapor_{amb}}$ are the water vapor partial pressures of the dehumidified and ambient air, and x is the water vapor molar fraction of the supplied air. The DOE also provides typical conditions at which to calculate the COP of the system: 90 °F ambient air at 90 % RH, with air delivered at 55 °F and 55 % RH.

The saturation pressures of water vapor at the ambient and supply conditions are 0.7 psi and 0.2 psi respectively, which gives a water vapor fraction of 0.028 and 0.0047 in units of kg water vapor per kg dry air. When inserted into the equation, the latent load is found to be 2.06 kJ/kg. This is therefore the minimum amount of work required to reduce the latent load to the specifications and this is also the minimum amount of energy required to regenerate the desiccant wheel. Additional energy losses occur due to unique material heat capacity, regeneration heat and temperature, inefficiencies in heat transfer, and process air latent/sensible conditions.

2.4.3 Desiccant Based Evaporative Cooling System COP

A simple schematic of a desiccant based evaporative cooling system is shown in Figure 2.4. Outside air is taken in to be processed at point 0, where it passes through a desiccant wheel (labelled B) from point 1 to 2. The process air then moves through a

heat exchanger wheel (C) and the first evaporative cooler (D), at which point the air is supplied to the room to be conditioned. Air passing through the room is then exhausted into a second evaporative cooler (F), a heat exchanger (C) and a heater which brings the air up to the regeneration temperature. Hot air passing through point 8 removes moisture from the desiccant wheel and it is exhausted at point 9. Using this diagram, an equation for the COP of the system can be formulated. In this case, $\dot{m}_p$ is the mass flow rate of the process air (points 0 through 4) and $\dot{m}_r$ is the mass flow rate of the regeneration air (points 5 through 9).

$$COP = \frac{\dot{m}_p\left(h_0 - h_4\right)}{\dot{m}_r\left(h_8 - h_7\right)}$$

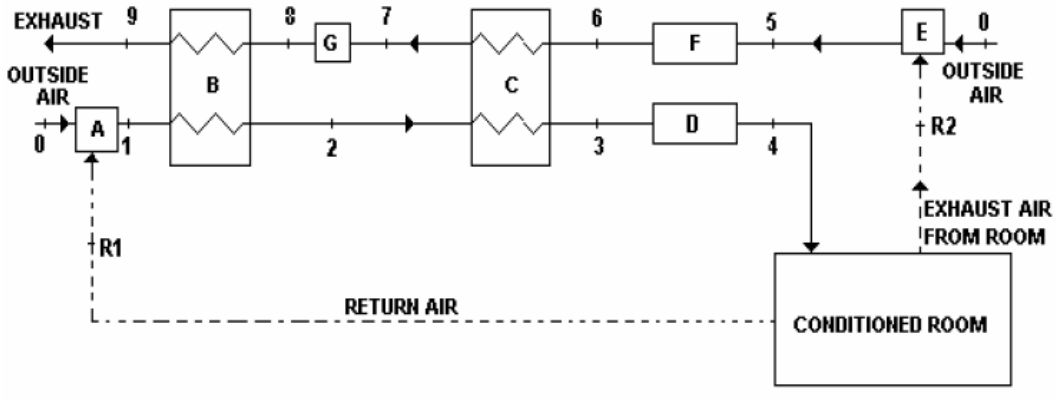

Figure 2.4: Schematic of a simulation used to estimate the COP of a desiccant evaporative cooling system [27]

Using a simulation based on a code developed by Camargo *et al.* [27], an estimate of the COP of a desiccant based evaporative cooling system can be determined. The code was modified to simulate both a temperature-sensitive desiccant and a conventional desiccant. The primary assumption made in this model is that the cooling or heat exchange achieved by the system is determined by a fixed effectiveness ε. Temperatures after the evaporative coolers are then determined by the difference between the process air and the wet bulb temperature of the process air. The wet bulb temperature is defined

as the lowest temperature that could be achieved by evaporating water in to a volume of air. Air at 100 % relative humidity, the wet bulb and the temperature of the air is the same as the air could not be cooled further by water evaporation.

$$T_3 = T_2 - \varepsilon_C\left(T_2 - T_6\right)$$

$$T_4 = T_3 - \varepsilon_D\left(T_3 - T_{3W}\right)$$

$$T_6 = T_5 - \varepsilon_F\left(T_5 - T_{5W}\right)$$

The results of the model are shown in Table 2.1. Camargo's model uses temperatures T_2 and T_9 based on experimental results. In the model used in this work, the temperatures are estimated based on energy balance on the desiccant wheel and takes into consideration the heating or cooling achieved by adsorbing or evaporating water from the desiccant material:

$$T_2 = T_1 + \frac{h_v(w_1 - w_2)}{c_{p-a}}$$

$$T_9 = T_8 - \frac{h_v(w_9 - w_8)}{c_{p-a}}$$

A COP of 0.52 is calculated based on a regeneration temperature of 115 °C, which is in close agreement to Camargo's original result of 0.45 COP at the same regeneration temperature and conditions. This is also in agreement with existing experimental results of desiccant enhanced evaporative cooling systems. Recent reviews have shown systems with COP ranging from 0.2 to 1 in various conditions.[28, 29]

Table 2.1: Conditions for COP Calculation

	T [°C]	w [kg/kg]	h [kJ/kg]
r	26.70	0.0151	65.36
0	31.00	0.0172	75.13
1	28.85	0.0161	70.12
2	49.28	0.0070	67.71
3	31.14	0.0070	49.22
4	18.54	0.0125	50.39
5	28.85	0.0161	70.12
6	23.37	0.0185	70.52
7	49.28	0.0185	97.49
8	115.00	0.0185	165.91
9	87.90	0.0315	172.30

Chapter 3

Experimental Design

The overall goal of the experimental design is to

1. Develop a high SR, low regeneration temperature desiccant based on a thermoresponsive polymer hydrogel
2. Experimentally demonstrate the feasibility of using a temperature-sensitive hydrogel as the substrate for a composite desiccant material
3. Use experimental data to investigate the potential energy savings that could be achieved by using a thermoresponsive polymer hydrogel based desiccant

3.1 Material Synthesis Parameters Investigation

3.1.1 Synthesis of LCST Hydrogel

Temperature sensitive gels were synthesized using Na-Alginate, NIPAM, MBAA, and α-ketoglutaric acid. First, 0.4667 g of Na-Alginate and 3.733 g of NIPAM were placed into 28 g of water and mixed on a stirring plate for 1 h. Next, 1 g each of a 0.15 wt.% solution of MBAA in water and a 0.48 wt.% solution of α-ketoglutaric acid was

mixed into the NIPAM/Alginate solution for 30 min. This solution was then placed into a vacuum chamber for 5 min to remove any dissolved air, and to eliminate any bubbles in the solution. The solution was then poured into a mold created by two glass slides separated by a 1.5 mm thick silicone rubber spacer. After being placed in the molds, the gels were exposed to 365 nm UV light for 12 h. After UV light exposure, the samples were placed into a DI water bath for 24 h to absorb water and maximize the porosity of the final gel. The gel sheets were then cut into 1 cm by 1 cm square samples. The samples were then frozen, freeze dried, placed in a salt bath, and freeze dried again. The freezing and salt bath steps were performed with some variations in order to determine the optimum combination of parameters. This NIPAM/Alginate hydrogel is based on a recipe that was developed by Zheng *et al*. [23]

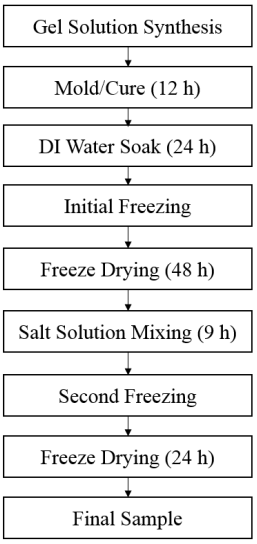

Figure 3.1: Flow chart of steps involved in desiccant synthesis

Initial freezing was accomplished either by placing the samples in the freezer section of a refrigerator for 12 h, or by immersing the samples in a dewar filled with liquid nitrogen (LN_2) for 1 h. The samples were then placed into a freeze drier to remove all water which left the samples with a porous structure that could easily be infiltrated by aqueous salt solution. The salt impregnation was accomplished by first creating a 5 wt.%

aqueous solution of LiCl or $CaCl_2$. Samples were placed into containers with 30 ml of salt solution, and then allowed to mix for 9 h, draining and re-filling the solution every 3 h. After salt impregnation, samples were freeze dried according to the previous method. A flow chart showing the steps involved in gel synthesis can be seen in Figure 3.1.

3.1.2 Synthesis of non-LCST Hydrogel

For reference, a non-LCST gel was synthesized using an acrylamide and alginate base. First, 73.96 g of DI water was mixed with 12 g of acrylamide and 2 g of alginate, along with 0.0072 g MBAA as a cross linker and 0.0204 g ammonium persulfate as a photo-initiator. This solution was then placed into a vacuum chamber for 5 min to remove any dissolved air, and to eliminate any bubbles in the solution. The solution was then poured into a syringe. A second mixture of 0.03 g TEMED, 0.26 g of $CaSO_4 \cdot 2H_2O$ and 12.04 was then mixed and poured into a second syringe. The two syringes were then connected and mixed by pumping the plungers back and forth 10 times. The solution was then poured into a plastic petri dish on a hotplate set to 50 °C and exposed to 254 nm UV light for 1 hour. The gel was then placed into a humid box for 24 h. Samples were then frozen, freeze dried, and impregnated with salt according to the procedure in Section 3.1.1.

3.1.3 Synthesis Parameters Comparison Testing

The swelling performance of the samples was tested using a sealed plexiglass chamber with a humidifier placed inside. A diagram of the setup is shown in Figure 3.2. The humidifier was turned on for 5 minutes in order to increase the humidity of the box. The chamber was then left alone for 1 h in order to allow the airborne water droplets to evaporate and settle, reducing the likelihood of water condensation on samples. Samples

to be tested were then placed on a plastic mesh on top of a petri dish and left inside the chamber for 12 h. Each sample was removed and weighed at 30 min intervals during the swelling process.

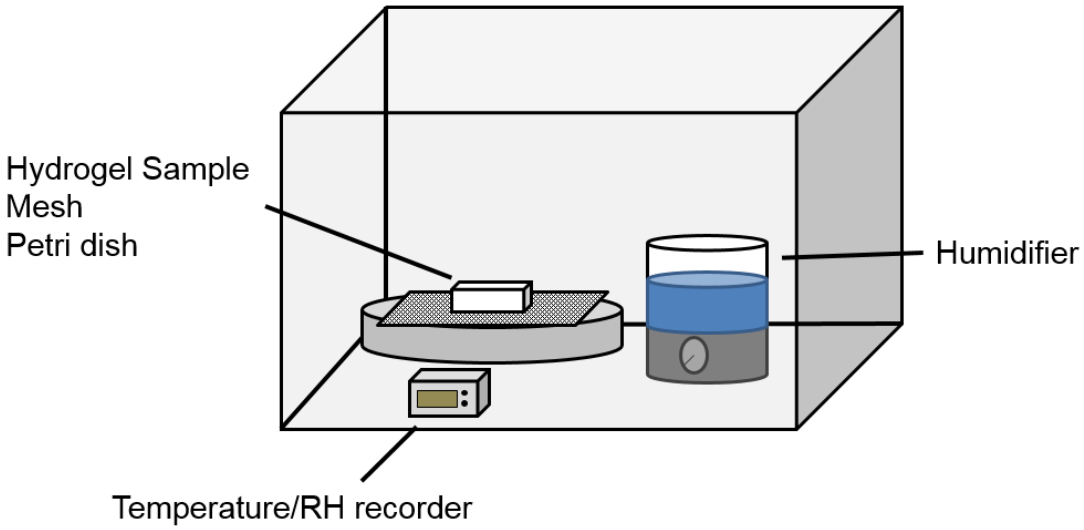

Figure 3.2: Diagram of the humidity box used for materials synthesis parameters investigation

3.2 Desiccant Adsorption Kinetics Testing

Water adsorption and regeneration kinetics were performed on LCST samples made from the best-performing synthesis recipe as determined by the process described in Section 3.1.3. Samples made from the non-LCST, acrylamide material were also tested.

A diagram of the experimental setup used to test material kinetics is shown in Figure 3.3. Tested samples were placed on a mesh platform suspended from a Denver Instruments SI-114 digital balance mounted over a test enclosure that was supplied air from a CSZ ZH-8-1-1-RH environmental chamber. The environmental chamber monitored the temperature and relative humidity through an RTD temperature sensor

and an Omega HX92BV0 relative humidity sensor placed in the test enclosure. The chamber uses a PID feedback loop controlled by a Watlow F-4 process controller to cool, heat, humidify and dehumidify the air sent to the test enclosure. Air was sent to the enclosure through flexible insulated hoses with a 12 VDC fan attached to the hose drawing air from the chamber. The test enclosure was constructed from extruded aluminum framing, acrylic sheet, and fiberglass insulation purchased from McMaster-Carr. Weight measurements from the digital balance were sent to a computer via serial port connection and recorded via RsCom software made by A&D Company, LTD. Data from the scale was recorded every 30 seconds. Temperature and humidity measurements were taken via a Sensirion SHTC-1 sensor through USB connection to computer.

Water vapor adsorption tests were conducted with air at 25 °C and 85-89 % relative humidity. A PTFE mesh platform suspended from a plastic bar with stainless steel wire was placed on the digital balance pan. Regeneration tests were conducted with air at 50 °C and 20 % relative humidity. A PTFE spray-coated copper mesh platform suspended from a plastic bar with stainless steel wire was placed on the digital balance pan. In both absorption and regeneration tests, the chamber was allowed to sit for 1 h in order to achieve steady state conditions and reduce the likelihood of water condensation on the sample or sample holder.

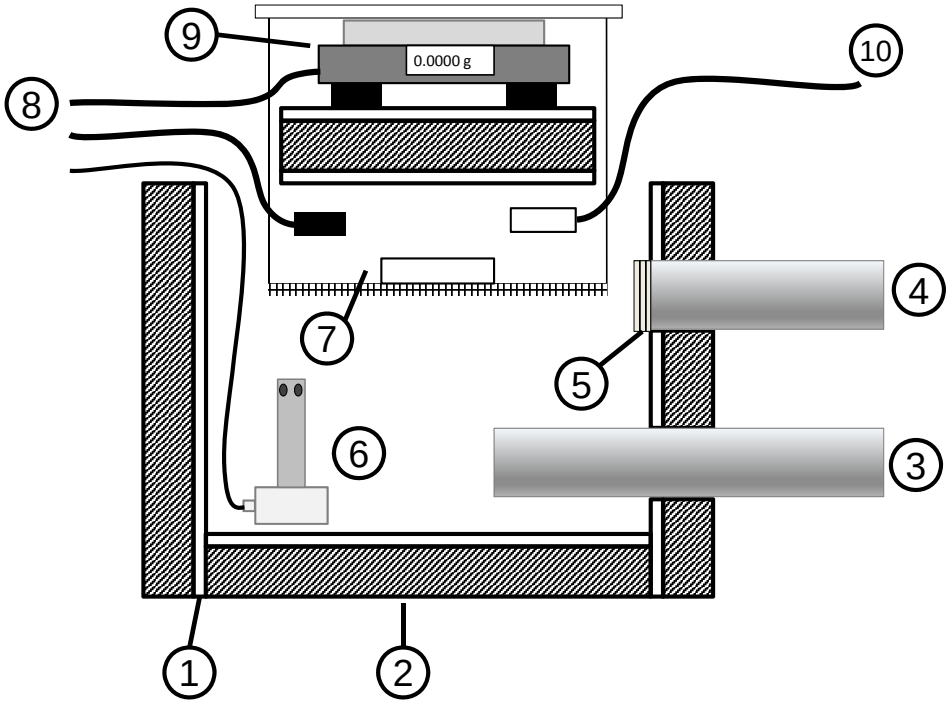

Figure 3.3: Diagram of the enclosure used to test absorption and regeneration behavior of gel samples 1. 1/4" acrylic sheet 2. Fiberglass insulation 3. Air return to environmental chamber 4. Air send from environmental chamber 5. Fan 6. Relative humidity sensor, output to environmental chamber 7. Sample on copper or PTFE mesh, supported by stainless steel wire to plastic bar placed on digital balance 8. Data serial output from scale, relative humidity and temperature sensor, to computer 9. Digital balance 10. Temperature sensor, output to environmental chamber

3.2.1 Cyclic Behavior

One concern with desiccant regeneration through water droplet formation and removal is that the desiccant salts that enable the water adsorption performance will be washed away. Hygroscopic salts adsorb water vapor through the formation of hydrates and salt solutions, but in conventional solid composite desiccant systems there is no loss of salt. Desiccant materials regenerated through water evaporation do not have the issue of salt washing away. Samples were subject to successive swelling and regeneration tests carried out according to the corresponding descriptions in Section 3.2. Samples

typically only achieved SR 2 in the adsorption test time (6 h) and conditions (RH 88-90 %). It was found that a SR $>$ 5 is necessary to achieve desiccant regeneration through water droplet formation through gravity. In order to reach the required SR after water adsorption experiments, samples were placed into the humid box shown in Figure 3.2, which has a RH level of $>$ 99 %. Samples in the humid box were measured periodically to determine when the critical weight had been achieve, typically 72-96 h after being placed in the chamber. Once sufficient water loading had been achieved, a regeneration test was performed on the sample.

Chapter 3, in part, has been submitted for publication of the material as it may appear in "Thermo-responsive desiccant with high adsorption capability and low regeneration temperature for energy efficient cooling." Cui, Shuang; Charles, Patrick; Chen, Renkun.

Chapter 4

Results and Analysis

4.1 Material Synthesis Parameters Results

The samples from the parametric study of synthesis factors were found to have notable differences in performance. Samples were compared by swelling ratio after 12 hours of absorbing water vapor in the humidity box per the procedure described in Section 3.1. The results of these tests are summarized in Figure 4.1. It was found that samples that were frozen by LN_2 post-salt impregnation performed worse than those frozen in a refrigerator. In general, the samples with $CaCl_2$ performed better than those impregnated with LiCl. Surface and cross-sections of the samples were also characterized using SEM imaging in order to better understand the factors which contribute to better swelling performance.

SEM analysis of the different synthesis techniques found significant differences in surface morphology between the different freezing methods. Samples that were initially frozen in the refrigerated freezer were found to have much larger pore size compared to the LN_2 frozen samples. It is possible that larger pores facilitated greater absorption of the salt solution, corresponding to improved swelling performance. LN_2 was chosen in

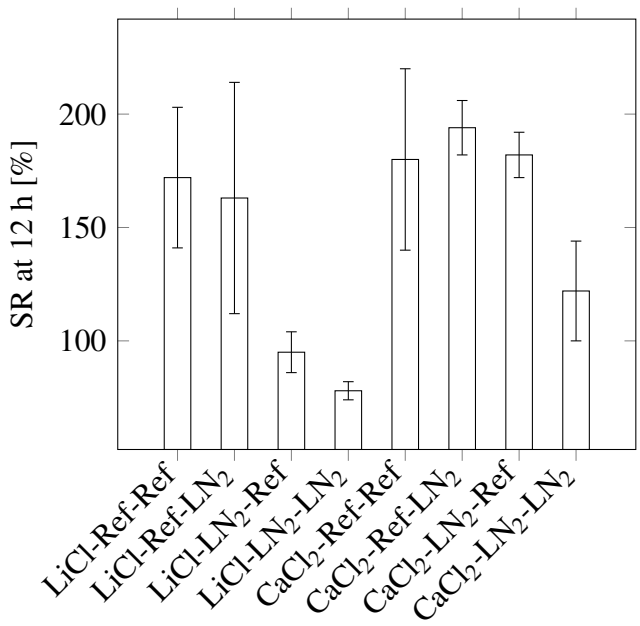

Figure 4.1: 12 hr SR data for different sample synthesis methods (Ref = refrigerator, LN_2 = liquid nitrogen

order to shrink the pores of the gel, and capture the salt inside the gel. The combination of $CaCl_2$-Ref-LN_2 was chosen as those samples consistently achieved the highest swelling ratios.

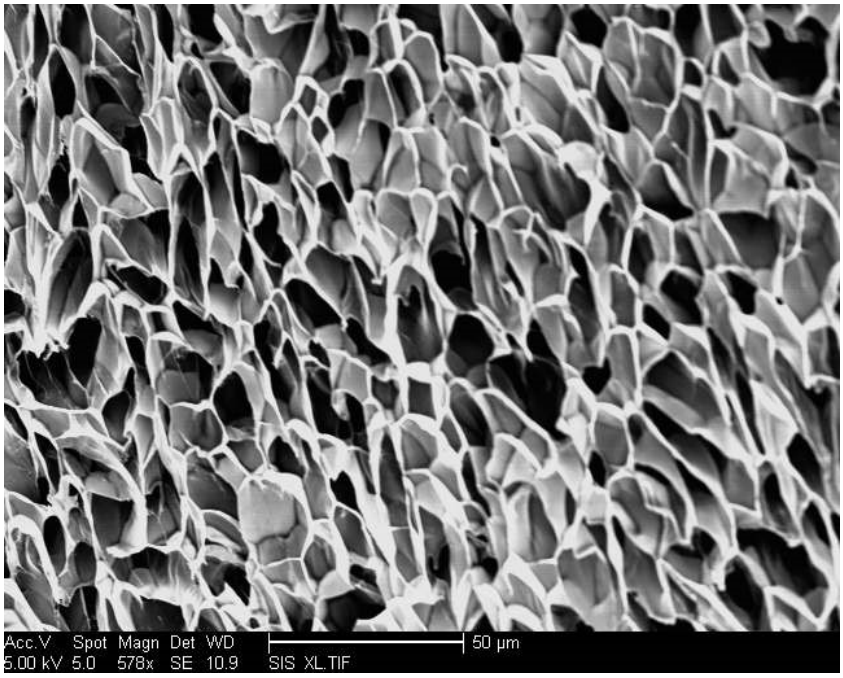

(a) Hydrogel material with initial LN_2 freezing

(b) Hydrogel material with initial refrigeration freezing

Figure 4.2: Microstructure of pores

4.2 Kinetics Testing Results

Data from the digital balance were found to have noise, equivalent to up to $\pm$ 4 mg error with the scale at steady state (no sample being tested). This was most likely due to vibration caused by the rotating fans and refrigeration system in the environmental chamber. In order to eliminate this noise, a 10-sample average (equivalent to 5 minutes) of the data was taken for the absorption tests, and a 4-sample average (2 minute) was taken for regeneration tests.

4.2.1 Swelling

A number of the tested samples achieved SR $>$ 2 in water adsorption kinetics testing. A summary of a selection of the samples tested, and their properties, are shown in Table 4.1 and plotted in Figure 4.3. Sample performance was found to have an inverse relationship with increasing salt loading. The problem of optimization of salt loading was discussed by Zhang *et al* [15], since hydrogel with too much salt will form a liquid layer which inhibits the adsorption of water vapor. In fact, Zhang found that at higher humidity levels (80-90%), this salt solution caused the desiccant wheel to overflow and the salt solution to drip off. In this work, the salt layer may have inhibited absorption by covering pores in the hydrogel material and reducing surface area exposed to the humid air. The lower salt loading may encourage absorbed water to stay in hydrogel material interior, rather than deliquesce on the surface of the hydrogel.

4.2.2 Regeneration

Samples in regeneration tests experienced water removal through droplet formation when the samples tested had achieved a threshold SR. The results from several

Table 4.1: Properties and Test Conditions for Tested Samples

Sample	Max SR	RH [%]	T [°C]	Sample Mass [mg]	Salt Mass [mg]	Salt Ratio
1	2.36	88 ± 1.1	24.5 ± 0.1	41.3	17.9	0.76
2	2.12	89 ± 1.3	24.5 ± 0.1	30.6	16	1.1
3	1.77	88 ± 1.0	24.5 ± 0.1	29.5	16.8	1.32

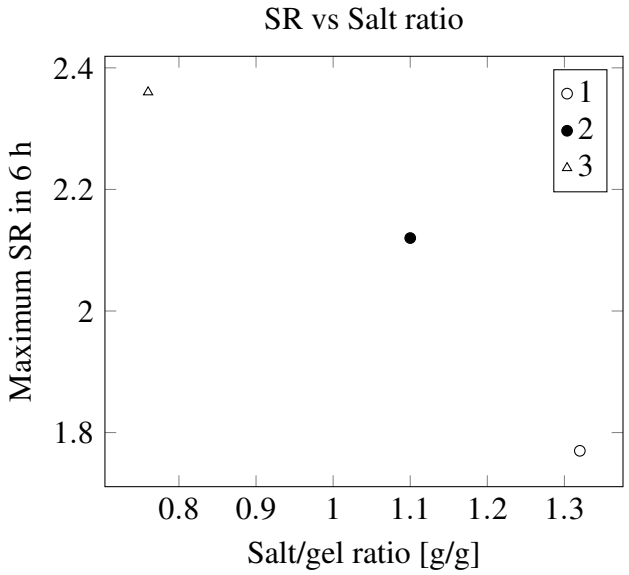

Figure 4.3: Swelling performance vs. salt loading, sample numbers reference Table 4.1

regeneration tests can be seen in Figure 4.4. In the figure, the water removal through droplet formation can be seen in the 'NIPAM Gel SR = 10' curve, where there is a sharp drop in water content in the first 10 minutes of the regen NIPAM samst.ples eration tethat had a SR of < 5 did not experience water removal through droplet formation. Visual observations indicated that of SR < 5 did experience LCST behavior with water beading on the surface or even water droplet formation, however the mass of the water dissolved from the sample was not of a sufficient mass to overcome the water droplet adhesion to the sample and sample holder. Droplet formation is mainly a function of the viscous force of water, adhesive forces of water to the sample and sample holder substrate, and the force of gravity on the water droplet mass. In order for a desiccant dehumidifier to

be regenerated by heating to LCST instead of water evaporation, the form factor of the dehumidifier must enable water droplet formation at the expected swelling ratio of the desiccant material. It is possible that on a larger scale, water expelled at LCST could cohere and reach the critical mass to form water droplets and run off from the desiccant material.

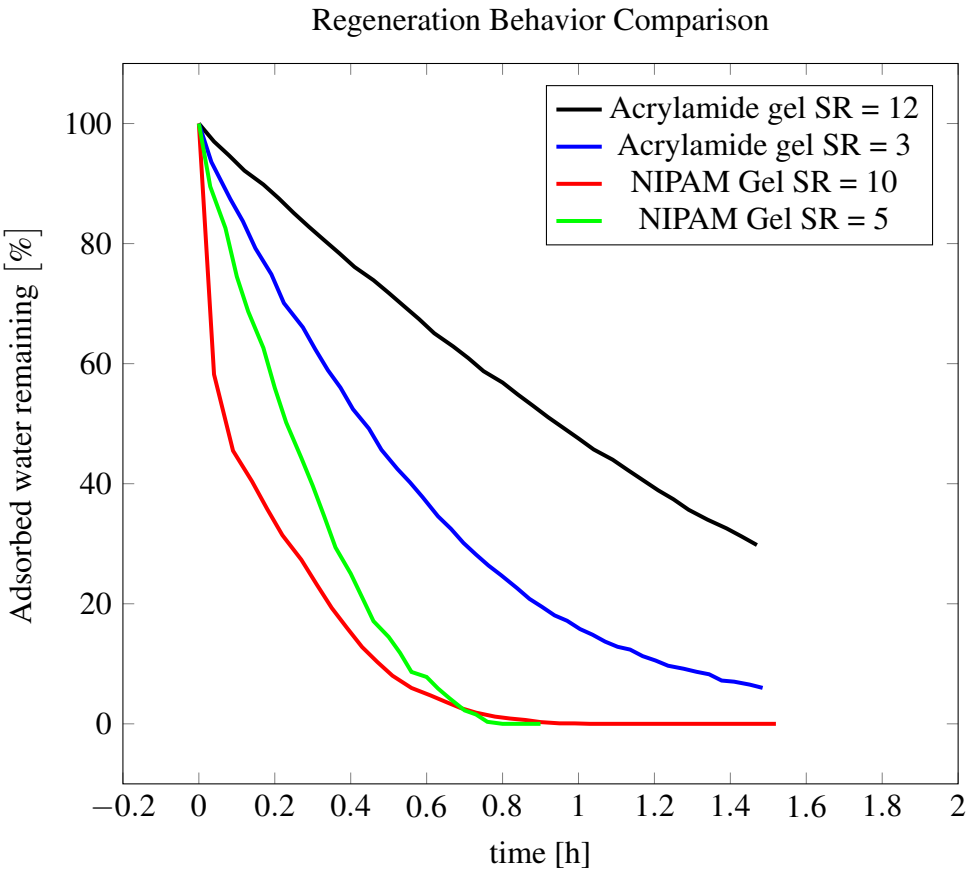

Figure 4.4: Regeneration kinetics curve for thermosensitive (NIPAM) and non-thermosensitive (acrylamide) hydrogel.

Tests were also performed to compare the regeneration behavior of a non temperature sensitive desiccant material. Even with a higher swelling ratio (SR = 12 in the most swollen sample tested), the non-thermoresponsive gel does not exhibit discontinuous mass loss when exposed to the same high temperature environment, and instead exhibits a characteristic water evaporation curve.

4.2.3 Cyclic Behavior

Samples that were subject to swelling and regeneration tests in serial experienced a reduction in desiccant performance. A plot of serial absorption tests performed after regeneration is shown in Figure 4.5. In one of the cyclic trials, a sample was originally loaded with 17.9 g salt. The sample lost 6.2 g of mass in the first regeneration and 5.6 g in the second regeneration. It is possible that the salt loss has a limit, but cyclic testing was limited to 3 trials in this work.

The $CaCl_2$ used in the samples is highly soluble in water, $\big($74.5 g/100ml water at 20 °C$\big)$. [30] Salt that is present on the surface or within the hydrogel matrix can be dissolved in the adsorbed water, which is then removed during the regeneration process. Samples with a SR < 5 that did not experience water droplet formation still experienced some salt loss. It was visually observed that samples that did not experience water loss through water droplets formation still released water from the hydrogel through deliquescence on the sample surface, so some water may have been transferred to the mesh supporting the sample instead of remaining on the sample, which contributed to some salt loss.

Table 4.2: Test Results for Cyclic Tested Sample

Mass of Hydrogel [mg]	Mass of hydrogel + salt [g]	Salt/Hydrogel ratio [g/g]	Max SR achieved in 6 h	RH [%]
23.4	41.3	0.76	2.36	88 $\pm$1.0
23.4	35.1	0.5	0.98	88 $\pm$0.8
23.4	29.5	0.26	0.69	87 $\pm$2.0

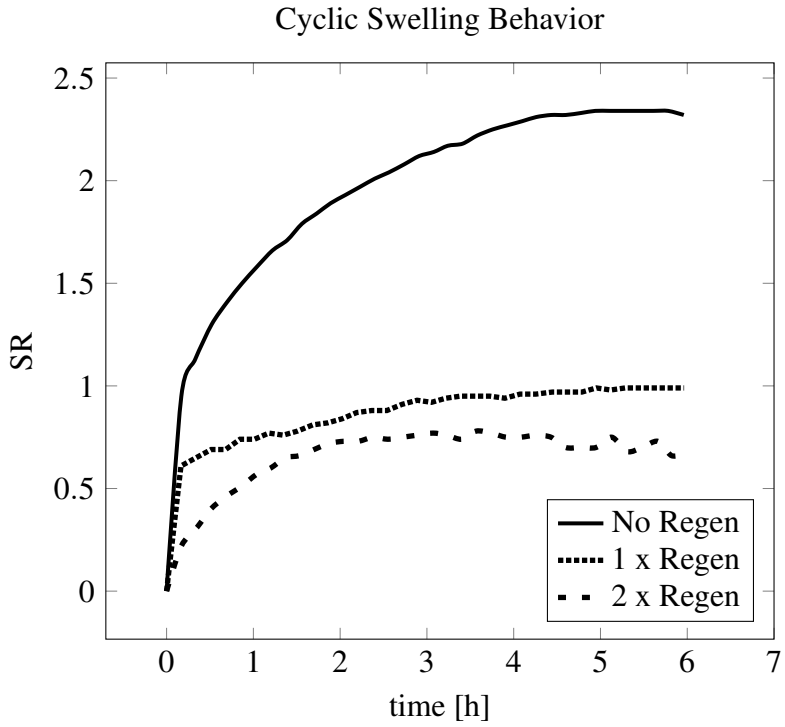

Figure 4.5: Adsorption test results from successive regeneration tests on thermo-responsive hydrogel

4.3 Thermodynamic Analysis of Temperature Sensitive Desiccant

Using the experimental performance results from the NIPAM hydrogel testing, a thermodynamic estimate of the minimum desiccant regeneration heat was calculated, similar to that which is shown in Section 2.4.2. In this case, the work needed to deliver this cooling benefit, W_{d-TR} is instead the energy required to raise the water-containing hydrogel up to its LCST temperature, at which point water will be released. In units of Joules per kg of desiccant hydrogel, we have:

$$W_{d-TR} = c_{p-TR}\left(T_{reg} - T_{amb}\right) + x_{d-sat}c_{pw}\left(T_{reg} - T_{amb}\right)$$

Variable x_{d-sat} is the average expected swelling ratio of desiccant material in use,

and c_{p-TR} is the specific heat of the desiccant material. Using 50 °C for T_{reg}, a value of 192.65 kJ/kg (mass of desiccant) is calculated. This number is still per mass of desiccant, so we must convert to mass of dry air delivered. The mass ratio of vapor reduction per mass of desiccant is $X_{d-a} = \frac{x_{v-amb} - x_{v-supp}}{x_{d-sat}}$ = 0.033, so the regeneration heat on a dry air delivered basis is then $Q_{regen} = X_{d-a} W_{d-TR}$ = 2.26 kJ/kg, which is just slightly greater than the theoretical limit for heat of regeneration of 2.06 kJ/kg for conventional desiccant materials found in Section 2.4.2.

The model utilized to estimate the COP of an evaporative cooling system in Section 2.4.3 can also be updated to give an estimate of increase in performance that might be achieved if this thermo-responsive material was used in a desiccant-enhanced cooling system. In this case, the regeneration temperature is lowered (55 °C vs 115 °C) and it is assumed that 50 % of the water is removed by water droplet formation, while the rest of the water is removed from the desiccant material by evaporation. The results of the model are shown in Table 4.3. The results indicate that the lower regeneration temperature results in a COP of 5.93, a significant improvement over systems using conventional desiccant material.

Table 4.3: Conditions for COP Calculation

	T [°C]	w [kg/kg]	h [kJ/kg]
r	26.70	0.0151	65.36
0	31.00	0.0172	75.13
1	28.85	0.0161	70.12
2	49.28	0.0070	67.71
3	31.14	0.0070	49.22
4	18.54	0.0125	50.39
5	28.85	0.0161	70.12
6	23.37	0.0185	70.52
7	49.28	0.0185	97.49
8	55.00	0.0185	103.45
9	41.41	0.0250	106.05

Chapter 4, in part, has been submitted for publication of the material as it may appear in ”Thermo-responsive desiccant with high adsorption capability and low regeneration temperature for energy efficient cooling.” Cui, Shuang; Charles, Patrick; Chen, Renkun.

Chapter 5

Conclusion

This work was successful in demonstrating a high absorption capacity desiccant material based on an LCST hydrogel-hygroscopic salt composite. This work was partially successful in demonstrating that the application of this composite material is feasible for use in a dehumidification system. It was found that the desiccant salt impregnated into the hydrogel was dissolved in the water that is removed when the material is raised to its LCST material. The high solubility of most salts presents a problem for the use of hygroscopic salts in desiccant materials regenerated through water loss at LCST. Thermodynamic analysis shows that LCST hydrogel materials are promising in reducing the energy cost of solid desiccant dehumidification systems. Investigation into methods of functionalizing polymer substrates to reduce the loss of desiccant salt in cyclic regeneration may also improve the outlook for these materials. If the material issues can be resolved, the use of a LCST hydrogel shows promise in the reduction of energy needed to dehumidify and cool air. Most significantly, this work estimates that an evaporative cooling system using an LCST desiccant material could reach a COP of up to 6 under typical air delivery conditions, an improvement over existing systems with a COP of 0.5 to 1.

5.1 Future Work

LCST hydrogel based desiccant materials have the potential to realize energy savings in HVAC systems if some of the challenges identified in this work can be overcome. One of the primary issues identified in this work is the loss of hygroscopic salt under cyclic testing. Hygroscopic salts may be appropriate for use, but in the current configuration the salt is washed away during the regeneration process. The use of a polyelectrolyte gel in the desiccant material could mitigate the loss of salt ions during the deswelling process. [31] It is also possible that a polymer-based desiccant that also exhibits LCST behavior could be bonded to the gel network in place of the hygroscopic salt. Another challenge is controlling the water removal through droplet formation. In the experiments shown in this work, a maximum of 50 % of water mass was removed through droplet formation. The rest of the water was removed through evaporation, which reduces energy savings.

A system level test is needed in order to experimentally determine the DCOP of the desiccant material. A schematic of a potential setup to measure the DCOP is shown in Figure 5.1. A fan draws humid air in from a humidifier, which is then sent through a block of the desiccant material. Serial absorption and regeneration tests can be run on the material to determine the dehumidification capacity of the material, as well as optimal flow rates for regeneration.

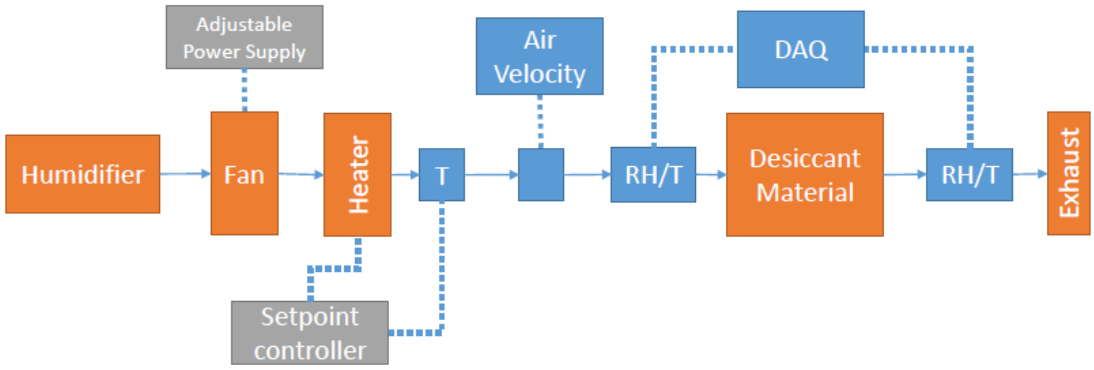

Figure 5.1: System schematic for determining DCOP of desiccant material

Appendix A

Desiccant Based Evaporative Cooling System COP Calculation Code

Script is written in MATLAB and is based on a model developed by Camargo et al. [27]

```
clc
clear all

%enthalpy calcs here: http://www.conservationphysics.org/
   atmcalc/atmoclc2.pdf
%verified using: http://www.daytonashrae.org/psychrometrics_si.
   html


%camargo code inputs
H = 500; %local Altitude  [m]
t0 = 31 ;%External temperature [  C ]
twb0 = 24; %External wet bulb temperature [  C ]
```

```
vp = 1.67 ;%Process air flow rate (m3/s)
tr1= 26.7;%return air temp (oC)
twbr1 = 21.52; %return air wet bulb reduce to 19 to match twb1
tr2 =  tr1;
twbr2 = twbr1;
x= 0.5; %("External Air mix (%): ")
t2 = 45; %guess t2
w2 = 0.00699; % ("Process air absolute humidity at the outlet (
   determined by desiccant wheel performance)
rp = 0.7 ;% ("Ratio of Return/Process air flow R/P

epsd = 0.9;% ("Effectiveness of Direct Evaporative Cooling: ")
epsi = 0.7;% ("Effectiveness of energy conservation wheel: ")

%pwc inputs
pgm_flag = 0;%0 for 55 regen, 1 for 115 regen
Q_abs = 3000 ; %head of adsorption on silica gel [J/kg] of
   water vapor (San et all 1993)
cp_d = 1000 ; %generic heat capacity for desiccant, matrix
   material [J/kg/K]
cp_v = 1996; %specific heat of water vapor at STP, [J/kg/K] ref
   : http://www.engineeringtoolbox.com/water-thermal-properties
   -d_162.html
h_v = 2257000; %latent heat of vaporization of water [J/kg] ref
   : http://www.engineeringtoolbox.com/water-thermal-properties
   -d_162.html
```

```
cp_w = 4918; %specific heat of water [J/kg/K] ref: http://www.
   engineeringtoolbox.com/water-thermal-properties-d_162.html
FF = 1; % factor to account for additional heat losses

if pgm_flag == 0;
    f_tr = 0.5; %fraction of water removed through water
       droplet formation, the rest is removed by evaporation
    t8 = 55 ;% Reactivation Temperature ( C) of thermo-
       responsive gel
else
    f_tr = 0; %fraction of water removed through water droplet
       formation, all is removed by evaporation
    t8 = 115; % Reactivation Temperature ( C) for silica gel
end

%LOCAL atmospheric pressure CALCULATION
P=101.325*(1-0.000025577*H)^5.2559 ; %local barometric pressure
    [kPa]

%return calc
br1   =(16.78*twbr1-116.9)/(twbr1+237.3); %saturation vapor
   pressure equation at temperature twb
% br1 = (10.19- 1730.63/(233.426 +tr1));
pswbr1   = exp(br1);
LR1   =(2.501-0.002361*tr1)*1000;
gamar1   =(cp_a_calc(tr1)*P)/(621.97*LR1);
pvr1   =pswbr1-(gamar1*(tr1-twbr1));
```

```
psr1 = .6112*exp(17.62*tr1/(243.12+tr1)); %saturation vapor
   pressure at wet bulb temp twb1 [Pa]
wr1 =  0.62197*(pvr1/(P-pvr1));
RHr1 = pvr1/psr1;
hr1 = (1.007*tr1 - 0.026) + wr1*(2501 + 1.84*tr1);


%ambient calc
b0   =(16.78*twb0-116.9)/(twb0+237.3); %saturation vapor
   pressure equation at temperature twb
pswb0   = exp(b0);
L0   =(2.501-0.002361*t0)*1000;
gama0   =(cp_a_calc(t0)*P)/(621.97*L0);
pv0   =pswb0-(gama0*(t0-twb0));
ps0 = .6112*exp(17.62*t0/(243.12+t0)); %saturation vapor
   pressure at wet bulb temp twb1 [Pa]
RH0 = pv0/ps0;

% pw0 = .6112*exp(17.62*twb0/(243.12+twb0)); %saturation vapor
   pressure at wet bulb temp twb1 [Pa]
% pv0 = pw0 - (0.00066*(1+0.00115*twb0)*(t0-twb0)*P);
w0   =0.62197*(pv0/(P-pv0));

h0 = (1.007*t0 - 0.026) + w0*(2501 + 1.84*t0); %state enthalpy
   calculation
```

```
%POINT 1 CALCULATION
% t1=(1-x)*tr1+x*t0 ; % pt 1 determined by mixing return air (
   pt r1) with outdoor air (pt 0) [C]
% twb1=(1-x)*twbr1+x*twb0 ;% pt 1 wb determined by return wet
   bulb air mix [C]
% ps1 = .6110*exp(17.62*t1/(243.12+t1)); %saturation vapor
   pressure equation at temperature t1 [kPa]
% pw1 = .6112*exp(17.62*twb1/(243.12+twb1)); %saturation vapor
   pressure at wet bulb temp twb1 [kPa]
% pv1 = pw1 - (0.00066*(1+0.00115*twb1)*(t1-twb1)*ps1);
% w1_pat   =0.62197*(pv1/(P-pv1)) ; %humidity ratio of air at
   pt 1, [kgwater/kgair]

t1=(1-x)*tr1+x*t0 ; % pt 1 determined by mixing return air (r1)
    with outdoor air (0)
twb1=(1-x)*twbr1+x*twb0; % pt 1 wb determined by return wet
   bulb air mix
b1   =(16.78*twb1-116.9)/(twb1+237.3); %saturation vapor
   pressure equation at temperature twb
pswb1   = exp(b1);
L1   =(2.501-0.002361*t1)*1000;
gama1   =(cp_a_calc(t1)*P)/(621.97*L1);
pv1   =pswb1-(gama1*(t1-twb1));
ps1 = .6112*exp(17.62*t1/(243.12+t1)); %saturation vapor
   pressure at t1 [kPa]
RH1 = pv1/ps1;
```

```
% pw1 = .6112*exp(17.62*twb1/(243.12+twb1)); %saturation vapor
   pressure at wet bulb temp twb1 [kPa]
% pv1 = pw1 - (0.00066*(1+0.00115*twb1)*(t1-twb1)*ps1); [kPa]
w1   =0.62197*(pv1/(P-pv1));

h1 = (1.007*t1 - 0.026) + w1*(2501 + 1.84*t1); %state enthalpy
   calculation



%POINT 2 CALCULATION
t2 = t1 +h_v*(w1-w2)/cp_a_calc(t2)/FF;
L2 = (2.501-0.002361*t2)*1000;
gama2 = (cp_a_calc(t2)*P)/(621.97*L2);
pv2  = (w2*P)/(0.62197+w2); %vapor pressure is known from pt 2
   humidity ratio
twb2   =  t2-0.1; %initialize wet bulb temperature as less than
    dry bulb
delta2 =  10; %intialize large error
while delta2 >=0.05
%     pswb2a =  0.6112*exp(17.62*twb2/(243.12+twb2)); %[kpa]
   calculate sat water pressure from wet bulb
%     pswb2b  = pv2 + (0.00066*(1+0.00115*twb2)*(t2-twb2)*ps2);
    %calc sat water pressure from wet bulb and vapor pressure
%     delta2  = abs(pswb2a-pswb2b);
%     twb2  = twb2-0.1;
```

```
    b2 = (16.78*twb2-116.9)/(twb2+237.3);
    pswb2a = exp(b2);
    pswb2b = pv2+(gama2*(t2-twb2));
    delta2 = abs(pswb2a-pswb2b);
    twb2 = twb2 -0.1;
end

ps2 = .6112*exp(17.62*t2/(243.12+t2)); %saturation vapor
   pressure at wet bulb temp twb1 [kPa]
RH2 = pv2/ps2;

h2 = (1.007*t2 - 0.026) + w2*(2501 + 1.84*t2); %state enthalpy
   calculation


% CALCULATION point 5
w5 = w1; %mixed outside air and exhaust return air
pv5  = (w5*P)/(0.62197+w5);
t5 =  x*tr2+(1-x)*t0;
twb5  =   x*twbr2+(1-x)*twb0;

ps5 = .6112*exp(17.62*t5/(243.12+t5)); %saturation vapor
   pressure at wet bulb temp twb1 [kPa]

h5 = (1.007*t5 - 0.026) + w5*(2501 + 1.84*t5);

% CALCULATION point 6
```

```
t6 =  t5-epsd*(t5-twb5); %temperature of post-evaporative
   cooler air
twb6  =   twb5; %by definition wet bulbs are the same, since
   air is cooled by as much as it can evaporate
b6 = (16.78*twb6-116.9)/(twb6+237.3);
pswb6 = exp(b6);
L6 = (2.501-0.002361*t6)*1000;
gama6 = (cp_a_calc(t6)*P)/(621.97*L6);
pv6 = pswb6-(gama6*(t6-twb6));

ps6 = .6112*exp(17.62*t6/(243.12+t6)); %saturation vapor
   pressure at wet bulb temp twb1 [kPa]

pw6 = .6112*exp(17.62*twb6/(243.12+twb6)); %saturation vapor
   pressure at wet bulb temp twb1 [kPa]
pv6_prime = pw6 - (0.00066*(1+0.00115*twb6)*(t6-twb6)*ps6);
w6 =  0.62197*(pv6/(P-pv6));

h6 = (1.007*t6 - 0.026) + w6*(2501 + 1.84*t6);

% CALCULATION point 3

t3 =  t2-epsi*(t2-t6); %t3 is determined by heat exchanger
   between prceoss and regen flow, depends on effectiveness of
   exchanger
w3 =     w2;
```

```
L3 = (2.501-0.002361*t3)*1000;
gama3 = (cp_a_calc(t3)*P)/(621.97*L3);
pv3 =  (w3*P)/(0.62197+w3);
twb3  =   t3-0.1 ;
delta3  = 10;
while delta3 >=0.05
%     pswb3a =  0.6112*exp(17.62*twb3/(243.12+twb3)); %
   calculate sat water pressure from wet bulb
%     pswb3b  = pv3 + (0.00066*(1+0.00115*twb3)*(t3-twb3)*ps3);
    %calc sat water pressure from wet bulb and vapor pressure
    b3 = (16.78*twb3-116.9)/(twb3+237.3);
    pswb3a = exp(b3);
    pswb3b = pv3+(gama3*(t3-twb3));
    delta3  = abs(pswb3a-pswb3b);
    twb3  = twb3-0.1;
end

ps3 = .6112*exp(17.62*t3/(243.12+t3)); %saturation vapor
   pressure at wet bulb temp twb1 [kPa]

h3 = (1.007*t3 - 0.026) + w3*(2501 + 1.84*t3);

% CALCULATION point 4

t4 =  t3-epsd*(t3-twb3); %process air is cooled by direct
   evaporation
```

```
twb4 =  twb3; %by definition wet bulbs are the same, since air
   is cooled by as much water as it can evaporate
b4 = (16.78*twb4-116.9)/(twb4+237.3);
pswb4 = exp(b4);
L4 = (2.501-0.002361*t4)*1000;
gama4 = (cp_a_calc(t4)*P)/(621.97*L4);
% ps4 = .6112*exp(17.62*t4/(243.12+t4)); %saturation vapor
   pressure equation at temperature t1 [kPa]
% pw4 = .6112*exp(17.62*twb4/(243.12+twb4)); %saturation vapor
   pressure at wet bulb temp twb1 [kPa]
% pv4 = pw4 - (0.00066*(1+0.00115*twb4)*(t4-twb4)*P);
pv4 = pswb4-(gama4*(t4-twb4));
w4 =  0.62197*(pv4/(P-pv4));

ps4 = .6112*exp(17.62*t4/(243.12+t4)); %saturation vapor
   pressure at wet bulb temp twb1 [kPa]
RH4 = pv4/ps4;

h4 = (1.007*t4 - 0.026) + w4*(2501 + 1.84*t4);

%
% CALCULATION point 7

t7= t6+((t2-t3)/rp);
w7 =  w6;
L7 = (2.501-0.002361*t7)*1000;
gama7 = (cp_a_calc(t7)*P)/(621.97*L7);
```

```
pv7  =  (w7*P)/(0.62197+w7);
% pv7 = pswb7-(gama7*(t7-twb7));
twb7  =   t7-0.1;
delta7  = 10;

while(delta7>=0.05)
%     pswb7a =  0.6112*exp(17.62*twb7/(243.12+twb7)); %[kpa]
   calculate sat water pressure from wet bulb
%     pswb7b  = pv7 + (0.00066*(1+0.00115*twb7)*(t7-twb7)*ps7);
    %calc sat water pressure from wet bulb and vapor pressure
    b7 = (16.78*twb7-116.9)/(twb7+237.3);
    pswb7a = exp(b7);
    pswb7b = pv7+(gama7*(t7-twb7));
    delta7  = abs(pswb7a-pswb7b);
    twb7  = twb7-0.1;
end

ps7 = .6112*exp(17.62*t7/(243.12+t7)); %saturation vapor
   pressure at wet bulb temp twb1 [kPa]

h7 = (1.007*t7 - 0.026) + w7*(2501 + 1.84*t7);

% CALCULATION point 8

w8 =  w7;
L8 = (2.501-0.002361*t8)*1000;
gama8 = (cp_a_calc(t8)*P)/(621.97*L8);
```

```
pv8  =  (w8*P)/(0.62197+w8);
twb8   =  t8-0.1;
delta8 =  10;

while delta8>=0.05
%     pswb8a =  0.6112*exp(17.62*twb8/(243.12+twb8)); %[kpa]
   calculate sat water pressure from wet bulb
%     pswb8b  = pv8 + (0.00066*(1+0.00115*twb8)*(t8-twb8)*ps8);
    %calc sat water pressure from wet bulb and vapor pressure
    b8 = (16.78*twb8-116.9)/(twb8+237.3);
    pswb8a = exp(b8);
    pswb8b = pv8+(gama8*(t8-twb8));

    delta8  = abs(pswb8a-pswb8b);
    twb8 =  twb8-0.1;
%     break
end

ps8 = .6112*exp(17.62*t8/(243.12+t8)); %saturation vapor
   pressure at wet bulb temp twb1 [kPa]
RH8 = pv8/ps8;

h8 = (1.007*t8 - 0.026) + w8*(2501 + 1.84*t8);

%CALCULATION point 9
eps_t9=10;
eps_t2=10;
```

```
t9=t8;
m_dot_a_p = vp*rho_a_calc(t1); %mass flow rate of process air [
   kg/s]
m_dot_a_r = m_dot_a_p*rp; %mass flow rate of process air [kg/s]
m_dot_v = m_dot_a_p*(w1-w2); %mass flow rate of absorbed water
   vapor [kg/s]
w_avg_p = (w2+w1)/2; %average humidity ratio between states 1
   and 2
w_avg_r = w8;


% while eps_t2 > 1
% eps_t2 = t1-t2+h_v*(w1-w2)/cp_a_calc((t2+t1)/2);
%
%
% eps_t2 = abs(eps_t2)
% t2= t2 +0.001;
% %     break
% end

%w9  =   w8-((w2-w1)/rp);
w9 = w8+(1-f_tr)*m_dot_v/m_dot_a_r;



while eps_t9 > 1
   eps_t9 = t8-t9-h_v*(w9-w8)/cp_a_calc((t8+t9)/2)/FF;
```

```
   eps_t9 = abs(eps_t9);
   t9 = t9-0.001;
end


% t9  =   t8-((t2-t1)/rp);

%w9 = w8;
L9 = (2.501-0.002361*t9)*1000;
gama9 = (cp_a_calc(t9)*P)/(621.97*L9);
pv9  =  (w9*P)/(0.62197+w9);

twb9   =  t9;
delta9 =  10;

while (delta9>0.05)
%     pswb9a =  0.6112*exp(17.62*twb9/(243.12+twb9)); %[kpa]
   calculate sat water pressure from wet bulb
%     pswb9b  = pv9 + (0.00066*(1+0.00115*twb9)*(t9-twb9)*ps9);
    %calc sat water pressure from wet bulb and vapor pressure
    b9 = (16.78*twb9-116.9)/(twb9+237.3);
    pswb9a = exp(b9);
    pswb9b = pv9+(gama9*(t9-twb9));

    delta9 =  abs(pswb9a-pswb9b);
    twb9 =  twb9-0.1
```

```
end

ps9 = .6112*exp(17.62*t9/(243.12+t9)); %saturation vapor
   pressure at wet bulb temp twb1 [kPa]
RH9 = pv9/ps9;

h9 = (1.007*t9 - 0.026) + w9*(2501 + 1.84*t9);

t_vect = [tr1,t0,t1,t2,t3,t4,t5,t6,t7,t8,t9];
t_vect_p = [26.7, 31, 28.85, 56.16, 32.78, 19.28, 28.85, 23.37,
    58.21, 115.5, 74.8];

twb_vect = [twbr1,twb0,twb1,twb2,twb3,twb4,twb5,twb6,twb7,twb8,
   twb9];
twb_vect_p = [21.52, 24, 21.83, 24.94, 17.78, 17.65, 22.76,
   22.76, 31.01, 41.2, 39];
w_vect = [wr1,w0,w1,w2,w3,w4,w5,w6,w7,w8,w9];
w_vect_p = [.0114, .016, .0135, .00699,.00699, .0120, .01607,
   .01847,.01847, .01847, .032];
p_vect = [pvr1,pv0,pv1,pv2,pv3,pv4,pv5,pv6,pv7,pv8,pv9];
h_vect = [hr1,h0,h1,h2,h3,h4,h5,h6,h7,h8,h9];
name_str = ['r','0','1','2','3','4','5','6','7','8','9'];


table = [t_vect; twb_vect;  w_vect;p_vect;h_vect];
fprintf('\tt [  C ] \t\ttwb [  C ]\tw [kg/kg]\tpv [kPa]\th [kJ/kg
   ]')
```

```
for i = 1:length(table(1,:))
    fprintf('\n%s\t',name_str(i))
    fprintf('%.2f \t\t%.2f \t\t%.4f \t\t%.4f\t\t%.2f\t\t%2.0f',
       table(:,i))
    fprintf('\t%s',name_str(i))
end
fprintf('\n ')
COP = (h0-h4)/(h8-h7)/rp;

fprintf('\n The COP of the system is %.2f \n',COP)

fprintf('\n pv6 \tpv6_prime')
fprintf('\n %.2f\t%0.2f \n',pv6, pv6_prime)
```

Bibliography

[1] C. T. Lewis, *An Elementary Latin Dictionary*. American Book Company, 1890.

[2] "2011 buildings energy data book," tech. rep., Pacific Northwest National Laboratory, 2012.

[3] D. Westphalen and S. Koszalinski, "Energy consumption characteristics of commercial building hvac systems volume I: Chillers, refrigerant compressors, and heating systems," tech. rep., Department of Energy, 2001.

[4] W. Goetzler, T. Sutherland, M. Rassi, and J. Burgos, "Research & development roadmap for next-generation appliances," tech. rep., Department of Energy, 2014.

[5] "Refrigerants environmental data: Ozone depletion and global warming potential," tech. rep., Linde Gases AG.

[6] G. J. M. Velders, D. W. Fahey, J. S. Daniel, M. McFarland, and S. O. Andersen, "The large contribution of projected hfc emissions to future climate forcing," *Proceedings of the National Academy of Sciences*, vol. 106, no. 27, p. 1094910954, 2009.

[7] W. Goetzler, R. Zogg, J. Young, and C. Johnson, "Non-vapor compression hvac report," tech. rep., Department of Energy.

[8] B. S. Davanagere, S. A. Sherif, and D. Y. Goswami *International Journal of Energy Research*, vol. 23, no. 2, pp. 103–116, 1999.

[9] V. C. Mei, F. C. Chen, Z. Lavan, R. K. Collier Jr., and G. Meckler, "An assessment of desiccant cooling and dehumidification technology," tech. rep., Oak Ridge National Laboratory, 1992.

[10] J. H. Dannies, "Solar air conditioning and solar refrigeration," *Solar Energy*, vol. 3, no. 1, pp. 34–39, 1959.

[11] B. C. Shelpuk and D. W. Hooker, "Development programmes in solar desiccant cooling for residential buildings," *International Journal of Refrigeration*, vol. 2, no. 5, pp. 173–179, 1979.

[12] T. S. Ge and J. C. Xu, *Advances in Solar Heating and Cooling*, ch. 13, pp. 329–379. Institute of Refrigeration and Cryogenics, 2016.

[13] Geibel Adsorber Inc., *Fundamentals for the regeneration of silica gel*, 2016.

[14] E. A. Levistkij, Y. I. Aristov, and M. M. Tokarev, "Chemical heat accumulators: A new approach to accumulating low potential heat," *Reaction Kinetics and Catalysis Letters*, vol. 59, no. 2, pp. 325–333, 1996.

[15] X. J. Zhang, K. Sumathy, Y. J. Dai, and R. Z. Wang, "Parametric study on the silica gel-calcium chloride composite desiccant rotary wheel employing fractal BET adsorption isotherm," *International Journal of Energy Research*, vol. 29, no. 1, pp. 37–51, 2005.

[16] C. X. Jia, Y. J. Dai, J. Y. Wu, and R. Z. Wang, "Use of compound desiccant to develop high performance desiccant cooling system," *International Journal of Refrigeration*, vol. 30, no. 2, pp. 345–353, 2005.

[17] S. Xu, L. Fan, M. Zeng, J. Wang, and Q. Liu, "Swelling properties and kinetics of $CaCl_2$/polyacrylamide hygroscopic hybrid hydrogels," *Colloids and Surfaces A: Physicochemical and Engineering Aspects*, vol. 371, no. 1, pp. 59–63, 2010.

[18] Y. Yang, D. Rana, and C. Q. Lan, "Development of solid super desiccants based on polymeric superabsorbent hydrogel composite," *RSC Advances*, vol. 5, no. 73, pp. 59583–59590, 2015.

[19] J. M. G. Cowie and V. Arrighi, *Polymers: Chemistry and Physics of Modern Materials*. CRC Press, 2008.

[20] E. O. Akala, P. Kopekov, and J. Kopeek, "Novel ph-sensitive hydrogels with adjustable swelling kinetics," *Biomaterials*, vol. 19, no. 11, pp. 1037 – 1047, 1998.

[21] H. He, X. Cao, and L. Lee, "Design of a novel hydrogel-based intelligent system for controlled drug release," *Journal of Controlled Release*, vol. 95, no. 3, pp. 391 – 402, 2004.

[22] J. Chen, M. Yoshida, Y. Maekawa, and N. Tsubokawa, "Temperature-switchable vapor sensor materials based on n-isopropylacrylamide and calcium chloride," *Polymer*, vol. 42, no. 23, pp. 9361–9365, 2001.

[23] W. J. Zhen, N. An, J. H. Yang, J. Zhou, and Y. M. Chen, "Tough alginate/poly(nisopropylacrylamide) hydrogel with tunable lcst for soft robotics," *ACS Applied Materials Interfaces*, vol. 7, no. 3, pp. 1758–1764, 2015.

[24] H. Yang, H. Zhu, M. M. R. M. Hendrix, N. J. H. G. M. Lousberg, G. de With A Catarina C Esteves, and J. H. Xin, "Temperature-triggered collection and release of water from fogs by a sponge-like cotton fabric," *Advanced Materials*, vol. 25, no. 8, p. 11501154, 2013.

[25] I. N. Tang and H. R. Minkelwitz, "Composition and temperature dependence of the deliquescence properties of hygroscopic aerosols," *Atmospheric Environment*, vol. 27, no. 4, pp. 467–473, 1993.

[26] "Building energy efficiency through innovative thermodevices funding opportunity announcement," tech. rep., Department of Energy.

[27] J. R. Camargo, E. Godoy, and C. D. Ebinuma, "An evaporative and desiccant cooling system for air conditioning in humid climates," *Journal of the Brazilian Society of Mechanical Sciences and Engineering*, vol. 27, no. 3, pp. 243–247, 2005.

[28] M. M. Rafique, P. Gandhidasan, S. Rehman, and L. M. Al-Hadhrami, "A review on desiccant based evaporative cooling systems," *Renewable and Sustainable Energy Reviews*, vol. 45, pp. 145 – 159, 2015.

[29] M. Sahlot and S. B. Riffat, "Desiccant cooling systems: a review," *International Journal of Low-Carbon Technologies*, vol. 11, no. 4, pp. 489–505, 2016.

[30] "Calcium chloride (anhydrous)," International Labour Organization, International Chemical Safety Cards Database.

[31] D. Melekaslan and O. Okay, "Swelling of strong polyelectrolyte hydrogels in polymer solutions: effect of ion pair formation on the polymer collapse," *Polymer*, vol. 41, no. 15, pp. 5737–5747, 2000.